

NUMERICAL HEAT TRANSFER STUDIES OF A LATENT HEAT STORAGE SYSTEM CONTAINING NANO-ENHANCED PHASE CHANGE MATERIAL

by

Ali Akbar RANJBAR*, **Sina KASHANI**, **Seyed Farid HOSSEINIZADEH**,
and Morteza GHANBARPOUR

Faculty of Mechanical Engineering, Babol Noshirvani University of Technology, Babol, Iran

Original scientific paper

UDC: 621.6.04:536.42

DOI: 10.2298/TSCI100412060R

The heat transfer enhancement in the latent heat thermal energy storage system through dispersion of nanoparticle is reported. The resulting nanoparticle-enhanced phase change materials exhibit enhanced thermal conductivity in comparison to the base material. The effects of nanoparticle volume fraction and some other parameters such as natural convection are studied in terms of solid fraction and the shape of the solid-liquid phase front. It has been found that higher nanoparticle volume fraction result in a larger solid fraction. The present results illustrate that the suspended nanoparticles substantially increase the heat transfer rate and also the nanofluid heat transfer rate increases with an increase in the nanoparticles volume fraction. The increase of the heat release rate of the nanoparticle-enhanced phase change materials shows its great potential for diverse thermal energy storage application.

Key words: nanoparticle, phase change material, solidification, thermal storage

Introduction

Because of the problems of fast depletion of conventional energy sources and ever increasing demand of energy, many researches all around the world started paying attention to renewable energy sources and energy storage systems. Energy storage is essential, whenever, the supply or consumption of energy varies independently with time. Basically there are three methods of storing thermal energy: sensible, latent, and thermo-chemical heat or cold storage. Thermal storage systems, based on the latent heat storage, have been relevant, especially in solar thermal applications. Solid-liquid phase change during heat storage and recovery processes provides considerable advantages such as high storage capacity and nearly isothermal behavior during charging and discharging processes. There are several promising developments going on in the field of application of phase change material (PCM) for heating and cooling of building. Zalba *et al.* [1] performed a detailed review on thermal energy storage that dealt with PCM, heat transfer studies, and applications. Farid *et al.* [2] also presented a review on the analysis of PCM, hermetic encapsulation, and application of PCM.

* Corresponding author; e-mail: ranjbar@nit.ac.ir

Mehling *et al.* [3] summarized the investigations and developments on using PCM in buildings. Kenisarin *et al.* [4] presented a review of investigations and developments carried out during the last 10-15 years in the field of PCM, enhancing heat conductivity, available fields of using PCM, and clarifying typical questions. Rajeev *et al.* [5] presented a numerical solution of inward solidification of phase change material contained in cylinder/sphere. Shen *et al.* [6] worked on thermal management of mobile devices. Their paper presented the experimental study of using phase change material in the cooling of the mobile devices. It investigated the thermal performance of transient charging and discharging of mobile devices in three different situations; making phone calls frequently, making long duration calls, and making occasional calls. The results showed that mobile devices are heated up fastest during the long duration usage. Ganaoui *et al.* [7] developed and qualified a numerical scheme coupling lattice Boltzmann and finite volumes approaches for test cases of phase change problems. Anandan *et al.* [8] presented a review of thermal management of electronics devices dealing with various aspects of cooling methods. During these years, researchers have tried to find new way to develop energy storage system. Using nano technology to increase the heat transfer shows great opportunity in storage system. Because of low thermal conductivity of conventional heat transfer fluids such as water, oil, and ethylene glycol mixture, nanotechnology is considered to enhance thermal characteristics with substantially higher conductivities. The presence of the nanoparticles in the fluids increases appreciably the effective thermal conductivity of the fluid and consequently enhances the heat transfer characteristics. Masuda *et al.* [9] reported on enhanced thermal conductivity of dispersed ultra-fine (nanosize) particles in liquids. Soon thereafter, Choi [10] was the first to coin the term “nanofluids” for this new class of fluids with superior thermal properties. Khanafer *et al.* [11] studied heat transfer enhancement in a two-dimensional enclosure utilizing nanofluids for various pertinent parameters. Khodadadi *et al.* [12] were the first to report on improved functionality of PCM through dispersion of nanoparticles. They found that the resulting nanoparticle-enhanced phase change materials (NEPCM) exhibit enhanced thermal conductivity in comparison to the base material. In this study the solidification behavior of the NEPCM and the various parameters affecting solidification in an enclosure were studied.

Problem statement

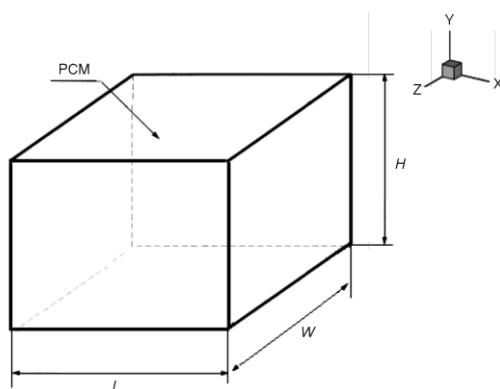


Figure 1. Geometry of the model

The analysis was carried out in two separate but related stages. Firstly, steady-state buoyancy driven convection in a differentially heated cavity containing a nanofluid was studied. Consider a 3-D cavity with adiabatic walls except left (T_h) and right (T_c) walls which are maintained at constant temperatures where $T_h > T_c$ (fig. 1).

Gravity acts parallel to the active walls pointing toward the bottom wall. The fluid is treated as an incompressible and Newtonian fluid. Thermophysical properties of the nanofluid are assumed to be constant, where as the density variation in the buoyancy

force term is handled by Boussinesq approximation. Thermophysical properties of the nanofluid is shown at tab. 1.

Table 1. Thermophysical properties of the nanofluid

	Copper nano-particles	Base fluid	Nanofluid $\phi = 0.025$	Nanofluid $\phi = 0.05$	Nanofluid $\phi = 0.1$	Nanofluid $\phi = 0.15$	Nanofluid $\phi = 0.2$
ρ [kgm ⁻³]	8954	997.1	1196.02	1394.95	1792.79	2190.64	2588.48
μ [kgms ⁻¹]	–	8.9·10 ⁻⁴	9.48·10 ⁻⁴	1·10 ⁻³	1.158·10 ⁻³	1.33·10 ⁻³	1.555·10 ⁻³
c_p [Jkg ⁻¹ K ⁻¹]	383	4179	3468.54	2960.67	2283.107	1851.64	1552.796
k [Wm ⁻¹ K ⁻¹]	400	0.6	0.648	0.698	0.8	0.915	1.04748
α [m ² s ⁻¹]	1.17·10 ⁻⁴	1.44·10 ⁻⁷	1.682·10 ⁻⁷	1.7·10 ⁻⁷	1.95·10 ⁻⁷	2.25·10 ⁻⁷	2.6·10 ⁻⁷
L [Jkg ⁻¹]	–	3.35·10 ⁵	2.72·10 ⁵	2.27·10 ⁵	1.68·10 ⁵	1.29·10 ⁵	1.03·10 ⁵
Ste	–	0.125	0.1275	0.1304	0.136	0.1435	0.150

Governing equation

Considering the nanofluid as a continuous media with thermal equilibrium between the base fluid and the solid nanoparticles, the governing equations are:

– Continuity

$$\frac{\partial u}{\partial x} + \frac{\partial v}{\partial y} + \frac{\partial w}{\partial z} = 0 \quad (1)$$

– X-momentum equation

$$\frac{\partial u}{\partial t} + u \frac{\partial u}{\partial x} + v \frac{\partial u}{\partial y} + w \frac{\partial u}{\partial z} = \frac{1}{\rho_{nf}} \left[-\frac{\partial p}{\partial x} + \mu_{nf} \nabla^2 u + (\rho\beta)_{nf} g_x (T - T_{ref}) \right] \quad (2)$$

– Y-momentum equation

$$\frac{\partial v}{\partial t} + u \frac{\partial v}{\partial x} + v \frac{\partial v}{\partial y} + w \frac{\partial v}{\partial z} = \frac{1}{\rho_{nf}} \left[-\frac{\partial p}{\partial y} + \mu_{nf} \nabla^2 v + (\rho\beta)_{nf} g_y (T - T_{ref}) \right] \quad (3)$$

– Z-momentum equation

$$\frac{\partial w}{\partial t} + u \frac{\partial w}{\partial x} + v \frac{\partial w}{\partial y} + w \frac{\partial w}{\partial z} = \frac{1}{\rho_{nf}} \left[-\frac{\partial p}{\partial z} + \mu_{nf} \nabla^2 w + (\rho\beta)_{nf} g_z (T - T_{ref}) \right] \quad (4)$$

– Energy equation

$$\begin{aligned} \frac{\partial T}{\partial t} + u \frac{\partial T}{\partial x} + v \frac{\partial T}{\partial y} + w \frac{\partial T}{\partial z} = \frac{\partial}{\partial x} \left[\frac{(k_{nf0} + k_d)}{(\rho c_p)_{nf}} \frac{\partial T}{\partial x} \right] + \\ + \frac{\partial}{\partial y} \left[\frac{(k_{nf0} + k_d)}{(\rho c_p)_{nf}} \frac{\partial T}{\partial y} \right] + \frac{\partial}{\partial z} \left[\frac{(k_{nf0} + k_d)}{(\rho c_p)_{nf}} \frac{\partial T}{\partial z} \right] \end{aligned} \quad (5)$$

The density of the nanofluid is given by:

$$\rho_{nf} = (1 - \phi)\rho_f + \phi\rho_s \quad (6)$$

whereas the heat capacitance of the nanofluid and part of the Boussinesq term are:

$$(\rho c_p)_{nf} = (1 - \phi)(\rho c_p)_f + \phi(\rho c_p)_s \quad (7)$$

$$(\rho\beta)_{nf} = (1 - \phi)(\rho\beta)_f + \phi\phi(\rho\beta)_s \quad (8)$$

with ϕ being the volume fraction of the solid particles and subscripts f, nf, and s stand for base fluid, nanofluid, and solid, respectively. The viscosity of the nanofluid containing a dilute suspension of small rigid spherical particles is given by:

$$\mu_{nf} = \frac{\mu_f}{(1 - \phi)^{2.5}} \quad (9)$$

whereas the thermal conductivity of the stagnant (subscript 0) nanofluid is:

$$\frac{k_{nf0}}{k_f} = \frac{k_s + 2k_f - 2\phi(k_f - k_s)}{k_s + 2k_f + \phi(k_f - k_s)} \quad (10)$$

The effective thermal conductivity of the nanofluid is:

$$k_{eff} = k_{nf0} + k_d \quad (11)$$

and the thermal conductivity enhancement term due to thermal dispersion is given by:

$$k_d = C(\rho c_p)_{nf} \sqrt{u^2 + v^2} \phi d_p \quad (12)$$

The empirically-determined constant C is evaluated following the work of Wakao *et al.* [13].

Also the latent heat that is evaluated using:

$$(\rho L)_{nf} = (1 - \phi)(\rho L)_f \quad (13)$$

Computational methodology

The numerical solution of the problem uses the enthalpy-porosity approach. By this approach, the porosity in each cell is set equal to the liquid fraction in that cell. Based on an enthalpy balance, the liquid fraction β is computed at each iteration. β takes the value $\beta = 1$ in the liquid phase, $\beta = 0$ in the solid phase and $0 < \beta < 1$ in the mushy zone (partially solidified region).

The governing equations are discretized using a control volume approach. For a typical run, the time step is 0.1 s and the number of sweeps for each time step is 400. The QUICK differencing scheme was used for solving the momentum and energy equations, whereas the PRESTO scheme was adopted for the pressure correction equation. The under-relaxation factors for the velocity components, pressure correction, thermal energy, and liquid fraction were 0.5, 0.3, 1, and 0.9, respectively. In enthalpy method, the solution is based on a fixed grid and governing equations are modified such that they are valid for both phases. Also the mushy zone constant was set to $10^5 \text{ kg/m}^3 \text{ s}$.

Validation of the model

Melting of gallium was simulated numerically by Brent *et al.* [14] with one vertical wall cooled while the opposite wall was heated. The top and bottom walls were adiabatic. The phase front propagation obtained in the present work is compared with their results in fig. 2. A reasonably good agreement is obtained.

The results of the recent work of Khanafer *et al.* [11] were used to benchmark the present computations for the case of natural convection of nanofluids within a differentially-heated square cavity. The predicted horizontal velocity component on the vertical mid-plane of the square cavity for the present study with a 81×81 grid system and that of Khanafer *et al.* [11] are compared in fig. 3 for $Gr = 10^4$ and 10^5 .

Regardless of the volume fraction of the nanoparticles, the well-established trends of the horizontal fluid velocity exhibiting accelerated flow near the horizontal walls and weak flow in the center of the cavity point to the observation that nanofluids behave more like a fluid [11] as opposed to flow of mm- or micron-size suspensions. The comparison for the cases of buoyancy-driven convection of a pure fluid (zero volume fraction) for the two Grashof numbers is excellent. According to Khanafer *et al.* [12], the dimensionless velocity was related to the inverse of the temperature difference between the two active walls. Consequently, the dimensionless velocity for $Gr = 10^5$ is lower compared to the corresponding $Gr = 10^4$ case. For a fixed Grashof number, as the loading of the nanoparticles is increased, “irregular and random” [11] motion of the nanoparticles promote greater momentum and energy transport throughout the cavity. Consequently, the extra thermal conductivity due to dispersion is enhanced. It should be noted that in the study of Khanafer *et al.* [11], both the Prandtl and Grashof numbers were evaluated using the properties of the base fluid. In our work, these dimensionless groupings were evaluated using the properties of the specific nanofluids. In effect, it appears that there are discrepancies between our predictions and those of Khanafer *et al.* [11] for non-zero solid volume fractions. The reader should not be alarmed on this matter in view of the different scaling parameters used to form the dimensionless groupings.

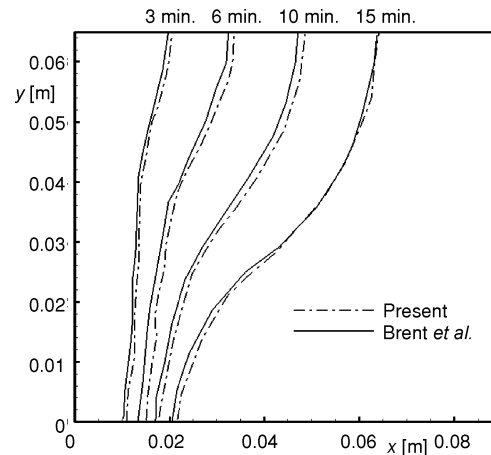


Figure 2. Progress of melting front with time: comparison among predictions of Brent *et al.* [14] and present work

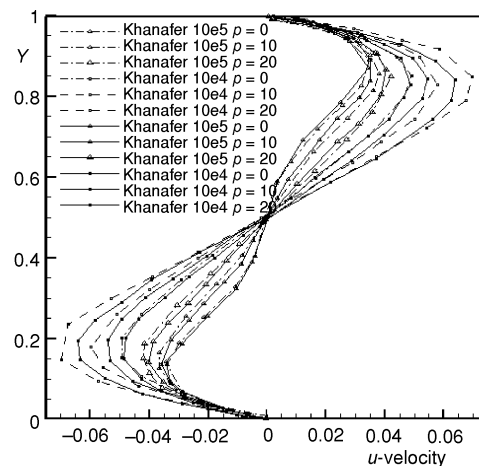


Figure 3. Comparison of the predicted horizontal velocity component on the vertical mid-plane of the square cavity for the present study and those of Khanafer *et al.* [11] with $Gr = 10^4$ and $Gr = 10^5$

The phase front for wall temperature of 15 °C at a time of 6 minutes was simulated numerically by Duan *et al.* [15] is shown in fig. 4, in order to investigate the effect of natural convection on the solidification of *n*-hexadecane. Also, fig. 5 shows the solid fraction vs. time for wall temperature of 15 °C. The numerical results agree very well with present work.

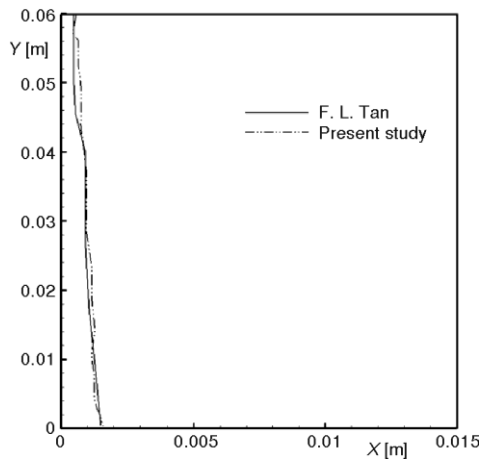


Figure 4. Phase front propagation at 6 minutes for wall temperature of 15 °C

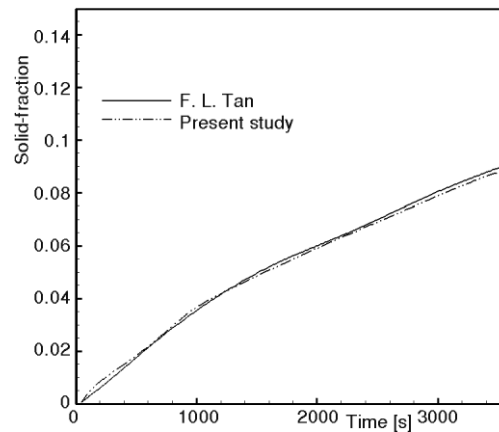


Figure 5. Solid fraction vs. time for wall temperature at 15 °C

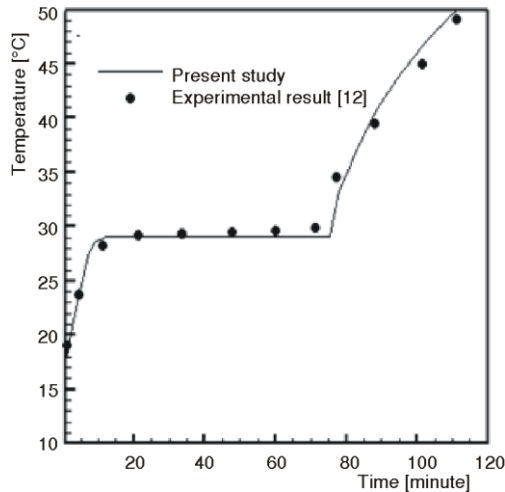


Figure 6. Variation with time of PCM's temperature at the centre of the rectangular container

From the results shown in fig. 6, it can be concluded that the agreement between present study and experimental data of Fuji and Zivkovic study [16] is well. In their study, a simple computational model for isothermal phase change material encapsulated in a single container was presented. As shown in fig. 6, the temperature of centre of the container increases until reach to the melting point. Then the PCM absorb energy to change phase from solid to liquid in a constant temperature, and finally, the temperature will increase rapidly again.

Following preliminary tests, a grid of 51^3 nodes in the fluid, selectively refined towards the walls, proved to yield an almost complete grid-independence of the results. Corresponding CPU times were of the order of 24 hours per test case on a 1500 MHz PC with 1024 megabytes RAM.

Results and discussion

Starting at time $t = 0$, the temperature of active left and right walls were held below the freezing temperature of the base fluid where the temperature of left wall is 273.15 °C and

the temperature of right wall is 283.15 °C. Consequently, the nanofluid will start freezing on the right wall and the solid front travels to the left. The remaining boundary conditions were unchanged in comparison to the conditions prior to $t = 0$. Colorized contours of the volume fraction of the nanofluid during freezing of the NEPCM at various time instants are shown in fig. 7 for wall temperature of 10 and 25 minutes for $Gr = 10^6$. It should be mentioned that the color red is used to identify the liquid phase, whereas color blue is indicative of the frozen solid phase.

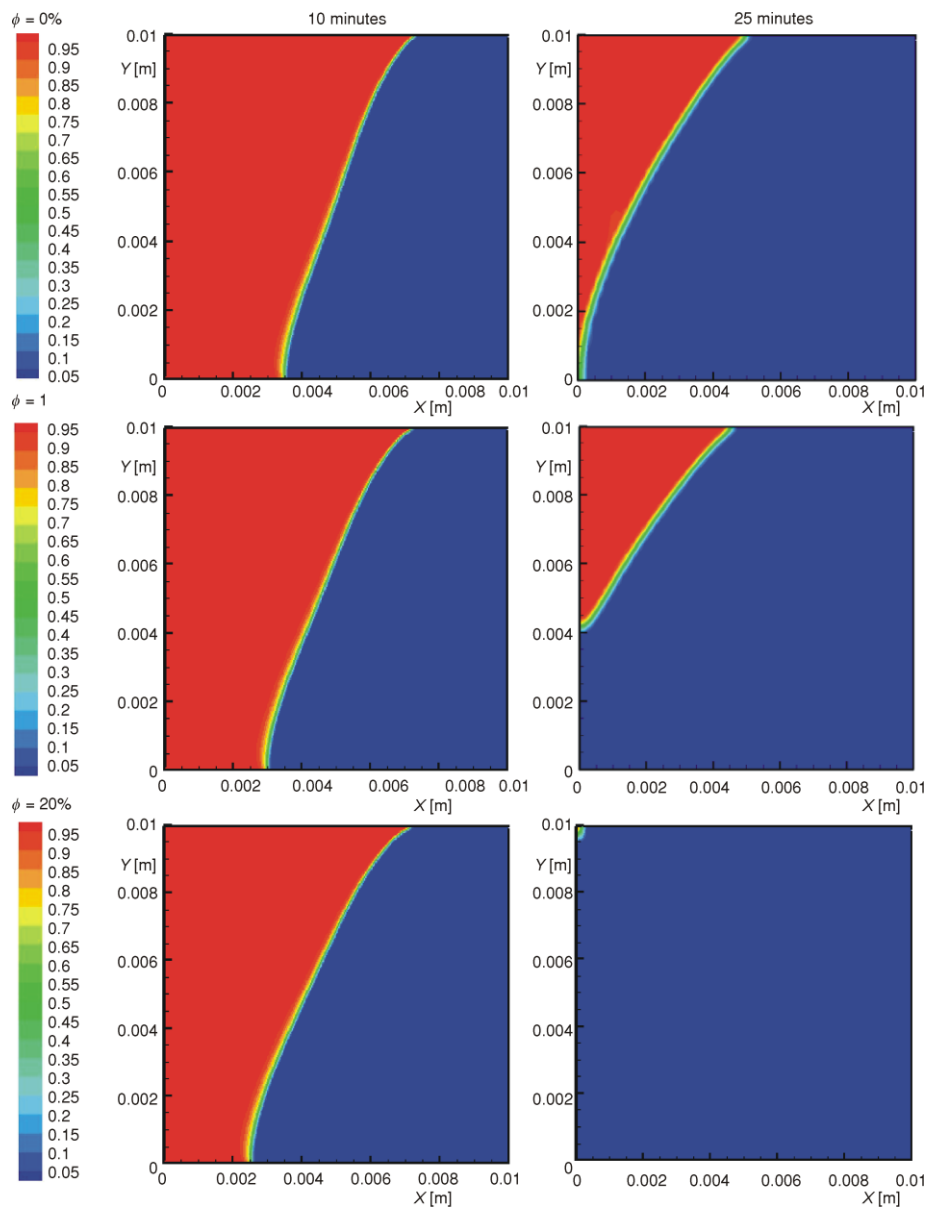


Figure 7. Colorized contours of the volume fraction of the nanofluid at $Gr = 10^6$
 (color image see on our to web site)

The instantaneous dimensionless volume of the nanofluid within the square cavity is presented in fig. 8 for all cases that were investigated. The liquid volume that continuously decreases from the start of the freezing exhibits little sensitivity to the value of the initial Grashof number except near the conclusion of the freezing process. On the other hand, the volume of the nanofluid is strongly dependent on the solid particle volume fraction of the dispersed nanoparticles. It is clear that because of the enhanced thermal conductivity of the nanofluid in comparison to that of the base liquid, by increasing the solid particle volume fraction the freezing time become lower.

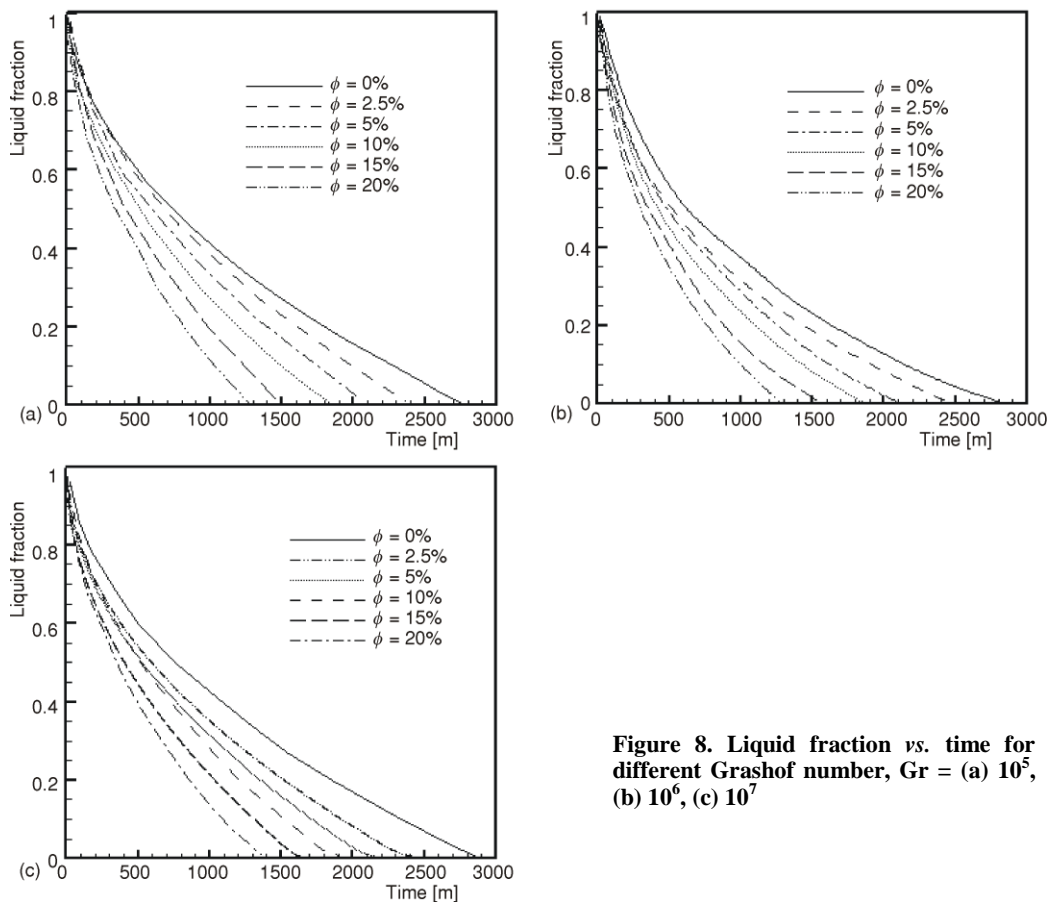


Figure 8. Liquid fraction vs. time for different Grashof number, Gr = (a) 10^5 , (b) 10^6 , (c) 10^7

In fig. 9 the temperature of the center line of the cavity is shown at different time at Grashof number of 10^5 . It can be seen that the temperature of the center line decreases by time and a significant drop occur near the cold wall. Also, in fig. 10 the temperature profiles of the center line of the cavity for two nanoparticle volume fractions are shown. It could be found from these figures that the effect of natural convection will descend by the time. This is because of the decrease in the liquid domain.

Figure 11 shows solid front at a certain time for three different Grashof numbers ($Gr = 10^5, 10^6, \text{ and } 10^7$). It is clear that natural convection effect descends by decreasing the Grashof number.

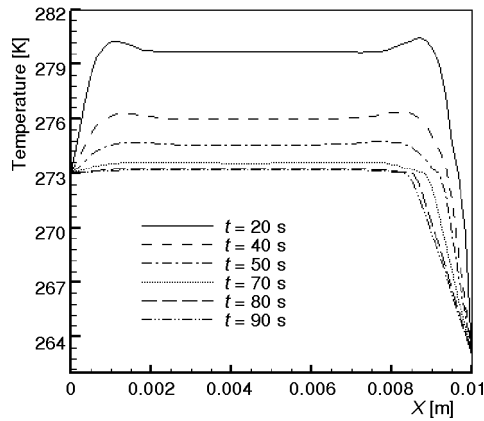


Figure 9. Temperature profile of the center line of the cavity at different times ($Gr = 10^5$)

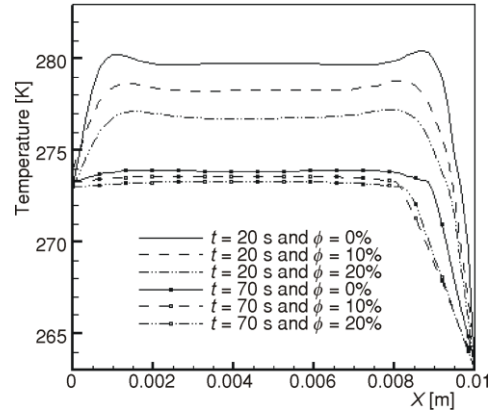


Figure 10. Temperature profile of the center line of the cavity for two nanoparticle volume fractions ($Gr = 10^5$)

The instantaneous streamlines within the nanofluid for the initial 10 s during the freezing of NEPCM for an initial $Gr = 10^5$, $Ste = 0.150$, and a solid particle volume fraction of 0.2 are shown in fig. 12. Also, to study the effect of natural convection, the streamlines within the nanofluid for various Grashof number are shown in fig.13. The streamlines at $t = 0$ correspond to a similar case studied by Khanafer *et al.* [11] and a clockwise rotating vortex is clearly observed. As a result of the sudden lowering of the temperatures of the two active walls at $t = 0$, the clockwise rotating vortex diminishes in strength and spatial coverage due to formation of a counter clockwise rotating vortex next to the left wall. The creation of the dual-vortex flow pattern was examined in greater detail by lowering the time step to 0.1 s for this case. Note that the formation, growth and equilibration of the counter clockwise vortex during the initial 10 s involves a dynamic interaction with the initially strong clockwise vortex. At the $t = 10$ s instant, two vortices rotating in opposite directions and nearly equal in size are observed squeezed between the left wall and a thin frozen layer next to the right wall. For the remainder of the freezing process, the dual-vortex structure will persist however due to the leftward movement of the freezing front, the vortices will shrink in coverage space and their strength will decay. It should be noted that the actual Grashof number for this unsteady freezing problem decreases with time due to the continuous shrinking of the distance between the left wall and the liquid-solid interface.

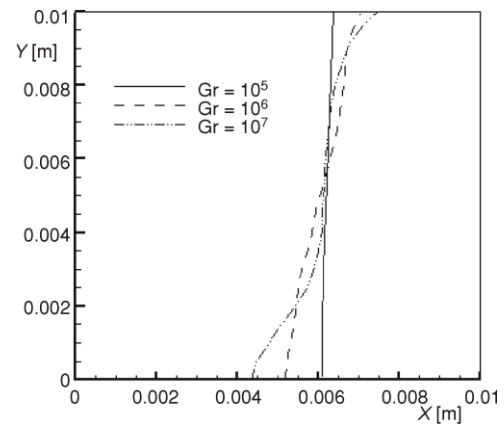


Figure 11. Phase front propagation at 6 minutes for wall temperature of $10\text{ }^\circ\text{C}$

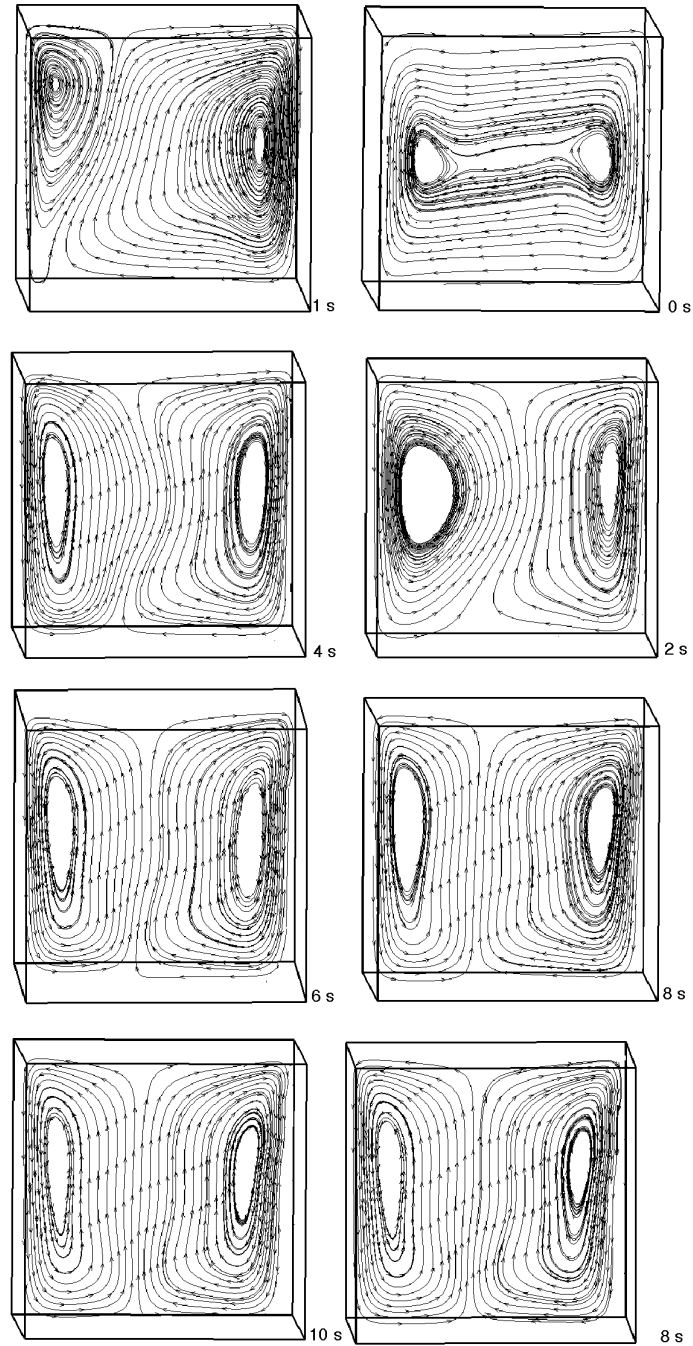


Figure 12. Streamline patterns at various time instants for the initial 10 s during the freezing of water with copper nanoparticles (solid particle volume fraction of 0.2) for an initial $Gr = 10^5$ and $Ste = 0.150$

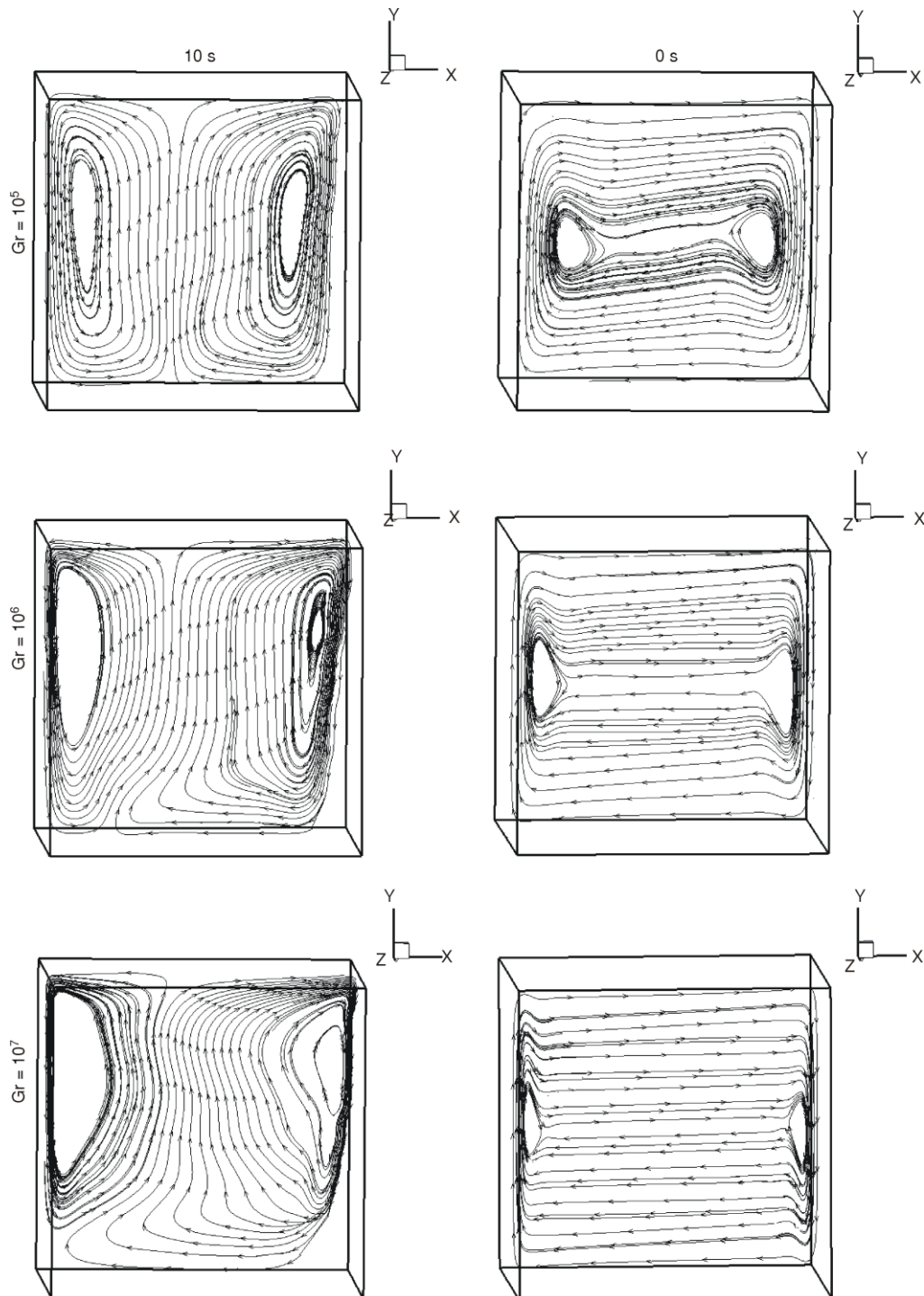


Figure 13. Streamline patterns at various Grashof number at $t = 0$ and 10 s during the freezing of water with copper nanoparticles (solid particle volume fraction of 0.2)

In order to study the temperature distribution in the domain, the temperature profiles along the middle of the enclosure for the six different nanoparticle volume fraction at 5 and 12 minutes are shown in fig. 14. There is a significant temperature drop in the solid region, with hardly any noticeable temperature difference in the liquid region. The liquid temperature is near the melting temperature of 273 K. This shows that the temperature gradient in the liquid is too small to cause a significant natural convection in the liquid. Thus, heat conduction is the dominant mode of heat transfer in both solid and liquid.

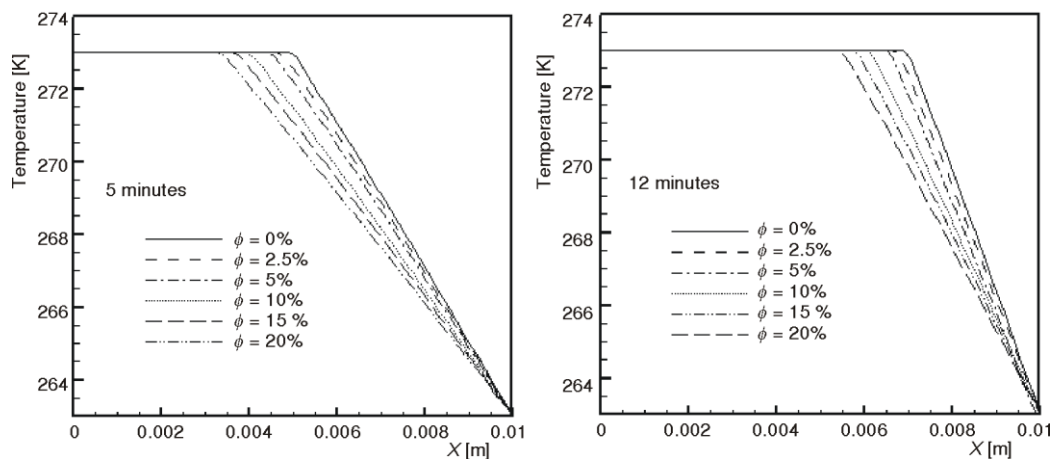


Figure 14. The temperature profiles along the middle of the enclosure

Conclusions

Solidification inside rectangular container has been studied numerically to investigate the effect of utilizing nanoparticle on the solidification phase front. The present results illustrate that the suspended nanoparticles substantially increase the heat transfer rate and also the nanofluid heat transfer rate increases with an increase in the nanoparticles volume fraction. Also, it was found that the temperature gradient in the liquid is too small to cause a significant natural convection in the liquid. Thus, heat conduction is the dominant mode of heat transfer in both solid and liquid.

Nomenclature

C – constant
 c_p – specific heat, [$\text{Jkg}^{-1}\text{K}^{-1}$]
 d_p – nanoparticle diameter, [m]
 f – liquid fraction
 Gr – Grashof number ($= \rho^2 g \beta \Delta T H^3 / \mu^2$)
 H – height of the enclosure, [m]
 k – thermal conductivity, [$\text{Wm}^{-1}\text{K}^{-1}$]
 L – latent heat of fusion, [Jkg^{-1}]
 p – pressure, [Pa]
 Pr – Prandtl number ($= \mu C_p / k$)
 T – temperature, [K]

t – time, [s]
 u, v, w – velocity components, [ms^{-1}]
 x, y, z – Cartesian co-ordinates

Greek letters

β – volumetric expansion coefficient, [K^{-1}]
 ε – constant
 μ – dynamic viscosity, [$\text{kgm}^{-1}\text{s}^{-1}$]
 ρ – density, [kgm^{-3}]
 ϕ – volume fraction of solid particles

Subscripts

ave	– average	l	– liquid
c	– cold	nf	– nanofluid
d	– thermal dispersion	ref	– reference
f	– based fluid	s	– solid
h	– enthalphy	0	– stagnant

References

- [1] Zalba, B., *et al.*, Review on Thermal Energy Storage with Phase Change Materials, Heat Transfer and Analysis and Applications, *Applied thermal Engineering*, 23 (2003), 3, pp. 251-283
- [2] Farid, M. M., Khudhair A. M., Al-Hallaj, S., A Review on Phase Change Energy Storage, Materials and Applications, *Energy Conversion Management*, 45 (2004), 9-10, pp. 1597-1615
- [3] Mehling, H., Hiebler, S., Review on PCM in Buildings-Current R&D, Paper Presented at the IEA Annex 17 Workshop in Arvika, Sweden, 2004, pp. 1597-1615
- [4] Murat, K., Khamid, M., Actual Problems in Using Phase Change Materials to Store Solar Energy, Paper Presentation at the NATO Advanced Study Institute Summer School on Thermal Energy Storage for Sustainable Energy Consumption (TESSEC), Cesme, Izmir, Turkey, 2005, pp. 6-17
- [5] Rajeev, K., Das, S., A Numerical Study for Inward Solidification of a Liquid Contained in Cylindrical and Spherical Vessel, *Thermal Science*, 14 (2010), 2, pp. 365-372
- [6] Shen, W., Tan, F.-L., Thermal Management of Mobile Devices, *Thermal Science*, 14 (2010), 1, pp. 115-124
- [7] El Ganaoui, M., Semma, E., A Lattice Boltzmann Coupled to Finite Volumes Method for Solving Phase Change Problems, *Thermal Science*, 13 (2009), 2, pp. 205-216
- [8] Anandan, S., Ramalingam, V., Thermal Management of Electronics: A Review of Literature, *Thermal Science*, 12 (2008), 1, pp. 5-26
- [9] Masuda, H., Ebata, A., Hishinuma, N., Alteration of Thermal Conductivity and Viscosity of Liquid by Dispersing Ultra-Fine Particles, *Netsu Bussei*, 4 (1993), 4, pp. 227-23
- [10] Choi, S. U. S., Enhancing Thermal Conductivity of Fluids with Nanoparticles, in: Developments and Application of Non-Newtonian Flows (Eds. D. A. Siginer, H. P. Wang), ASME, FED-Vol. 231/MD-Vol. 66, 1995, pp. 99-105
- [11] Khanafer, K., Vafai, K., Lightstone, M. L., Buoyancy-Driven Heat Transfer Enhancement in a Two-Dimensional Enclosure Utilizing Nanofluids, *Int. J. Heat Mass Transfer*, 46 (2003), 19, pp. 3639-3653
- [12] Khodadadi, J., Hosseinizadeh, S. F., Nanoparticle-Enhanced Phase Change Materials (NEPCM) with Great Potential for Improved Thermal Energy Storage, *Int. J. Comm Heat Mass Transfer*, 34 (2007), 5, pp. 534-543
- [13] Wakao, N., Kagueli, S., Heat and Mass Transfer in Packed Beds, Gordon and Breach Science Publishers, New York, USA, 1982, pp. 175-205
- [14] Brent, A. D., Voller, V. R., Reid, K. J., Enthalpy-Porosity Technique for Modeling Convection-Diffusion Phase Change: Application to the Melting of a Pure Metal, *Numer Heat Transfer*, 13 (1988), 3, pp. 297-318
- [15] Duan, Q., Tan, F. L., Leong, K. C., A Numerical Study of Solidification of n-Hexadecane Based on the Enthalpy Formulation, *Journal of Materials Processing Technology*, 120 (2002), 1-3, pp. 249-258
- [16] Zivkovic, B., Fulii, I., An Analysis of Isothermal Phase Change of Phase Change Material within Rectangular and Cylindrical Containers, *Solar Energy*, 70 (2001), 1, pp. 51-61